Influence Of Initial Compaction Conditions On Shrink-Swell Behavior During Drying Wetting Paths.

Derfouf Feth-Ellah Mounir [(1)], Taïbi Saïd [(2)], Abou-Bekr Nabil [(1)], Allal Mohamed Amine [(1)]
1 Laboratoire Eau et Ouvrages dans Leur Environnement, Université Abou-Bekr Belkaïd, Faculté de Technologie, BP 230, Tlemcen, 13000 Algérie.
2 Laboratoire Ondes et Milieux Complexes, CNRS UMR 6294, Université du Havre, 53 rue de Prony, 76058 Le Havre, Cedex, France.

Abstract

This paper presents an experimental study carried out on clay used in the core of Boughrara dam (North West of Algeria). The characterization of the volumetric behavior under the effect of suction is studied on drying wetting paths which highlight the correspondence between void ratio, degree of saturation, and water content versus suction. The initial conditions correspond to statically compacted specimens at different initial water contents and dry densities. The test results showed that at constant water content, the drying wetting path was independent of the initial dry density. On the other hand, the drying wetting path was found greatly influenced by initial water content. On drying path, specimens with high initial water content, tend to shrink more, and for suction higher than 30MPa, the drying path was found to be independent of initial conditions. On wetting path, the swelling potential was found dependent on the dry density more than the water content.

Keywords*: Compaction, Drying, Wetting, Soil suction, Shrinkage, Swelling.*

1. Introduction

Unsaturated soils are usually defined as mixture of tree phases: solid liquid and gaz. In such soils, the contractile skin would be subjected to the water pressure u_w, which is lower than the air pressure u_a. The difference pressure (u_a-u_w), is referred to as suction, or more precisely: matric suction.

For these soils, the soil–water characteristic curve (SWCC) represents a constitutive relationship. In other words, the soil water characteristic curve describes the relationship between soil suction (S) and soil water content (w), or degree of saturation (Sr), on drying or wetting paths. Knowing the specific density of the soil ($Gs= \gamma_s/\gamma_w$), the associated changes in void ratio (e) versus suction can be determinated. Various properties of unsaturated soils can be derived from the SWCC curve: shear strength, hydraulic conductivity, volume changes, ([25], [7], [18]). Also, parameters like the air entry value (S_e), shrinkage limit, can be obtained from the SWCC (figure 1), and used to obtain fitting parameters to model the SWCC curve ([20], [6]).

As the soil moves from a saturated state to drier condition or vise versa, soil volume changes by shrinking on drying path or swelling on wetting path. As a result, many problems and damages can be caused the existing constructions ([11], [1]).

For compacted soils, because of their large using in construction of different soil structures such as roads, railroad embarkments, earth dams, many researches were undertaken in other to better understand their behavior on drying wetting path. These studies have highlighted the influence of compaction stress, compaction water content and dry density, clay mineralogy on such paths ([28], [16], [27], [30], [10], [29]).

The shrinkage curve (drying path) of a soil specimen shows different phases of deformation. From a progressive drying of natural saturated soil, [29] distinguished two phases: (i) normal shrinkage, and (ii) residual shrinkage. [4]and [12], add a third phase at the begin of shrinkage curve called structural shrinkage. Figure 1 shows a general form of the shrinkage curve in diagram [e-w], where we have also localized the position of the air entry value, the shrinkage.

Similar to the multiphase shrinkage behavior of a soil specimen, the swelling of desiccated soils also occurs in three different phases ([26]), namely primary swelling, secondary swelling, and no swelling.

In this paper, we propose to study the behavior of Boughrara clay dam compacted at the optimum Proctor conditions (SPO), on drying wetting path, and to bring out the influence of variations in the initial compaction conditions in terms of water content and dry density on such path.

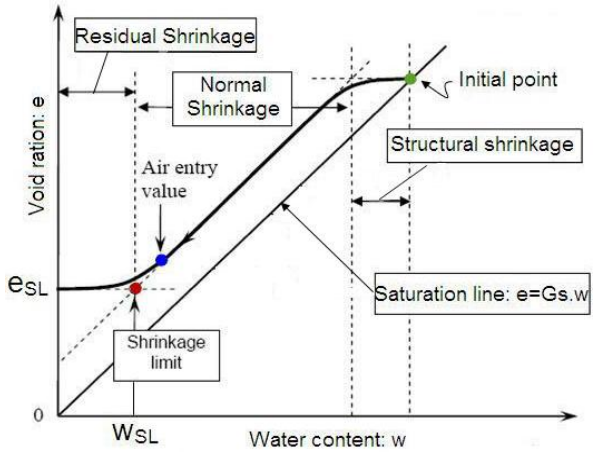

Figure 1.Three phases of a shrinkage curve (i.e., Haines, 1923) along with several key characteristics associated with the soil properties.

2. Material and methods

Tested material was taken from the deposit soil used for the construction of Boughrara core Dam, located in the North West Algeria, at about 60 km for Tlemcen city. The identifications test results are shown in tables 1 and 2.These results showed a predominance of the clay fraction. 70% of the elements are less than 2 µm, and the methylene blue index (MBI) is 10.11. This material is characterized by high plasticity and little activity (Ac). From the calcium carbonate content ($CaCO_3$) value and the specific surface area (SST), we can deduce that this is marly clay composed mainly of Kaolinite and Illite. According to the USCS/LPC classification, this clay is designated: CH: highly plastic clay with low organic percentage

2.1. Osmotic technique for control of suction

This technique is based on the osmotic principle. The difference between two solutions having different concentrations and separated by a semi-permeable membrane induces a difference between the pressures of the two solutions. This difference is the osmotic pressure. The sample is made in contact within an aqueous solution of polyethylene glycol (PEG) by semi-permeable membrane which is characterized by a specific value of MWCO (Molecular Weight Cut Off). Since PEG molecules cannot cross the semi-permeable membrane, suction is applied to the water through the membrane by osmosis and its value is controlled by the concentration of the PEG solution.

The relationship between suction (S) and PEG concentration (C_{PEG}) was firstly established by [17], and completed by [23] up to 10MPa. This relationship was found independent from the type of PEG, and it can be approached by a parabolic equation: $S=11C_{PEG}^2$, where the suction is expressed by (MPa), and the concentration of PEG by (g/g water). In this study PEG 20000 and 6000 were used to impose soil suction between 50kPa to 8000kPa by using respectively a semi permeable membrane with MWCO 12000 Da and 3500 Da.

Figure 2 shows a photo of the device performed for this technique. It is to set the semi-permeable membrane into a beaker containing PEG solution through a PVC O-ring. This last, is then slipped on to the walls of the beaker until the contact between the solution and the membrane is perfect (no air bubbles trapped under the membrane). The beaker is then covered by parafilm membrane to prevent evaporation from samples.

However, it is necessary to note certain points that have to be carefully taken in uses this technique:

- The temperature intervenes in the calculation of the osmotic potential which is the suction developed by the solution. It is, therefore, necessary to work at constant temperature (20°C in our case).
- The volume of osmotic solution may increase (on drying path), or decrease (on wetting path); this induces the variation of the solution concentration. In order to avoid this effect, we must use a great deal of solution.

Table 1. Physical properties of Boughrara clay.

Granulometry					Plasticity			Specific density	Optimum Proctor	
<80µm	<2µm(2)	D60	D30	D10	w_L	w_P	Ip(1)	γ_s/γ_w	γ_d	w
97%	72%	1µm	0.7µm	0.6µm	54%	26%	28%	2.65	16.2 kN/m^3	21%

Table 2. Chemical properties of Boughrara clay.

$CaCO_3$	MBI	SST	Organic Content	Ac (1/2)
20%	10.11	212 m²/g	5-6.5%	0.39

- The chemical instability of cellulosic membrane results in its decomposition in acidic environment or under the bacterium effect in soil. To solve this problem, one can add to the osmotic solution some drops of antibiotic (penicillin), or a spoon of Benzoic acid.
- According to [31], it is necessary to wait two days between the preparation and use of solution, in order to allow stabilization of solution density.

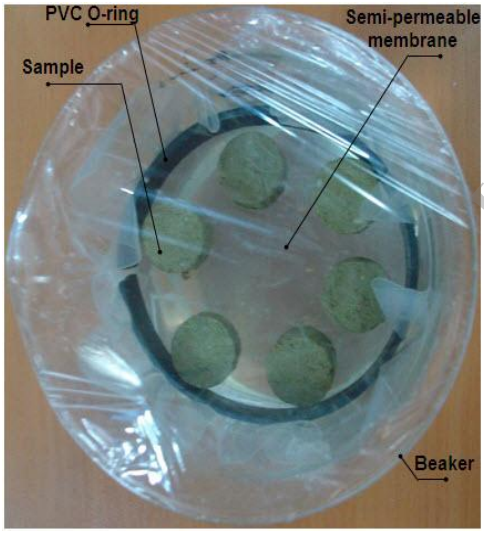

Figure 2. Device of osmotic technique

2.2. Vapor equilibrium technique for control suction

Total suction can be imposed on an unsaturated soil specimen by controlling relative humidity (RH) of the atmosphere surrounding the soil. Humidity can be controlled by using aqueous solutions ([23], [19]).

A soil specimen is placed in a closed thermodynamic environment (container or desiccator) containing an aqueous solution of a given chemical compound (figure 3). Depending on the physico-chemical properties of the compound, a given RH is imposed within the sealed environment. This technique is generally used to impose very high suction range which can reach 1000MPa ([19]).

Water exchanges occur by vapour transfer between the solution and the specimen, and the given suction is applied to the specimen when vapour equilibrium is achieved. Consequently, this technique is considered extremely time consuming.

NaCl, KCl, $(NH_4)2SO_4$, $MgCl_26H_2O$, KOH, H_2SO_4 were used as saturated salt solutions to impose suction between 20 MPa and 500 MPa, and distilled water was used to impose zero suction value.

When humidity is controlled by using solutions, as activity of the solutions is very sensitive to thermal fluctuation, temperature must be strictly controlled during testing. In our case, all desiccators were placed at 20C°.

2.3. Time of stabilisation

By measuring the variation of the sample mass, the time of stabilisation is obtained. The equilibrium is reached when the sample mass remains constant. With this method, we have estimated that the time equilibrium for vapour equilibrium technique exceed 50 days, where, for the osmotic technique it range between 15 and 20 days.

2.4. Experimental program and Samples preparation

The experimental program consist of two types of tests: Drying and wetting tests and oedometer free swell tests. The preparation of the test specimens was carried out in three steps as follows:

In the first step, natural soils were air-dried, and the aggregates were carefully crushed.

In the second step, the required quantity of water was added to the soil and both were carefully mixed (by spraying). The soil-water mixture was kept in a sealed plastic bag for at least 24 h to achieve uniform moisture conditions.

In the third step, the materials were statically compacted at desired dry density and water content.

For samples used in drying wetting tests, a special mould was used. The obtained specimens were 22mm in diameter and 12 mm in height. Immediately, they were put in the different devices used for these tests. In this case, each point corresponds to a different specimen, which can offer the advantage of shorter test duration.

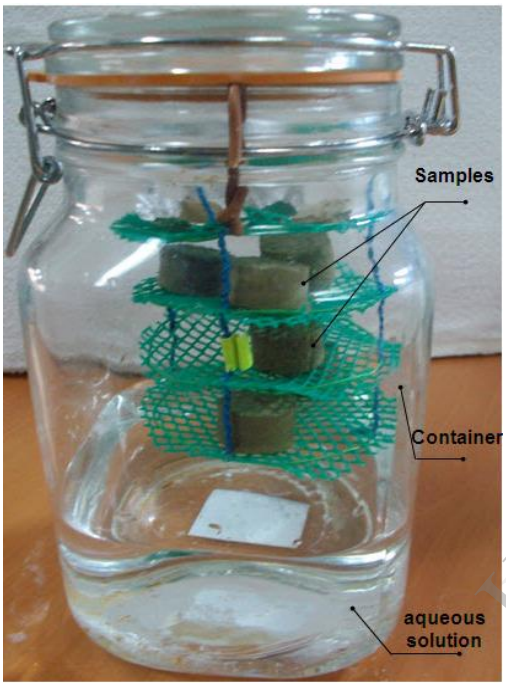

Figure 3. Device of vapour equilibrium technique.

Compaction parameters were determined by Standard Optimum Proctor (SPO). For the present study, five compaction conditions were chosen. These are;

- Maximum dry density and optimum moisture content (SPO, γ_d=16.2 kN/m^3, w=21%),

Dry side

- Maximum dry density and 3% dry of optimum moisture content (SPO-3, γ_d=16.2kN/m^3, w=18%),
- 98% of maximum dry density and 3% dry of optimum moisture content (98%SPO-3, γ_d=15.88kN/m^3, w=18%),

Wet side

- Maximum dry density and 3% wet of optimum moisture content (SPO+3, γ_d=16.2kN/m^3, w=24%),
- 98% maximum dry density and 3% wet of Optimum moisture content (98%SPO+3, γ_d=15.88kN/m^3, w=24%).

Compaction curve and the compaction conditions are shown in Figure 3. Table 3 present the soil state parameters of these initial conditions.

The initial suction of compacted materials were determined by using the filter paper method ([2]). The calibrated filter papers (Whatman42) were placed in the specimens during compaction, protected on both sides by ordinary filter papers, between two soil layers. Measured values are also presented in Table 3. From the initial suction, the sample follows a drying path if imposed suction is higher than the initial one, in the opposite case, it follows a wetting path.

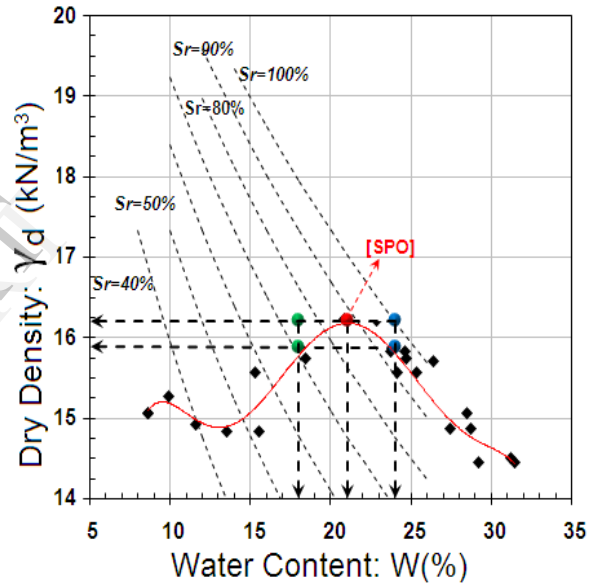

Figure 4. Compaction curve and compaction conditions.

For the same initial conditions (table 3), a free swell oedometric tests were undertaken, according to the ASTM norms ([3], method A). In this test, the specimen is lowed to swell under token pressure (1kPa, in our case) by submerging the specimen in distilled water. After attaining an equilibrium condition, the soil specimen is then loaded and unloaded following the conventional oedometer test procedure. Samples were compacted directly in the oedometer ring, to a height of 15mm and 50mm in diameter.

Table 3. Compaction conditions of soil specimens

Initial conditions	Initial Suction S_i (kPa)	w_i(%)	γ_d(kN/m3)	e_0	Sr_i(%)
SPO (*)	700	20.68	16.36	0.62	88.49
SPO (**)	757	21	16.2	0.636	87.5
SPO-3(*)	1045	18.07	16.27	0.629	76.12
98%SPO-3(*)	870	18.07	15.92	0.665	72.06
SPO+3(*)	237	23.7	16.31	0.625	100
98%SPO+3(*)	93	24.2	15.98	0.658	97.46
(*) Static compaction, (**) Dynamic compaction-Proctor test-					

3. Results and discussion

Figure 5 and 6 represent drying wetting path on compacted Boughrara clay. The three graphs in the right-hand side (B, D, E) show the changes in void ratio, degree of saturation and water content with logarithm of suction. On the left-hand side, the void ratio (A) and degree of saturation (C) are plotted versus water content. This presentation was chosen in other to highlight the correspondence between the curves and the different phases in the behavior of the soil. A suction of 1 kPa, correspond really to null suction.

3.1. Drying wetting path for SPO specimens

In figure 5, the first graph (A) is the usual shrinkage-swelling curve, with the void ratio as a measure of the external volume.

On the drying path, the void ratio decreases as the water is extracted from soil. When the water content reaches shrinkage limit w_{SL}, the void ratio tends to a constant value, noted e_{SL}. The value of w_{SL} is about 12% and e_{SL} is 0.37. In this case, we can identify two phases in the shrinkage path: normal shrinkage and residual shrinkage (figure 1). The absence of the structural shrinkage phase is due to the fact that the soil is initially unsaturated (The initial point is located to the left of saturation line, $Sr_i \approx 90$ %). According to [Fredlund and Rahardjo, 1993], in this state, water phase is continuous and air phase is occlude in bubbles.

The second graph (B) is the compressibility plot, where the effective stress is replaced by suction. Two phases are distinguished. The first is characterized by large variation of the void ratio when suction is increased, and in the second, this variation becomes negligible. The transition suction between the two domains, S_{SL}=4MPa, is termed the "shrinkage limit suction", and correspond to w_{SL} in graph (A). Beyond this value, the liquid phase becomes mainly discontinuous, and is located in the menisci around the contact points. At microscopic level, this behavior is explained by the changes in the obliquity of inter-granular forces with respect to the normal to the contact between the grains, ([13], [16]).

The evolution of the degree of saturation with water content is represented in the graph (C). The normal and the residual shrinkage phase are also identified in this plane. The evolution of the degree of saturation in these two phases can be approached by straight lines with two different slopes. There intersection, correspond to shrinkage limit, w_{SL}.

The two last graphs (D and E) represent respectively the SWCC curve. It appears that the effect of suction on the void ratio is widely related to the saturation of the material. The maximum compressibility is occurs when the water content is less than the shrinkage limit, w_{SL} (i.e., normal shrinkage phase). Beyond this value, the degree of saturation falls below the value of 75% to reach about 40 % at a suction value of 500 MPa. In this interval, the decrease in water content is approximately 7 %.

The wetting path of specimens compacted to the SPO conditions, shows a linear variation in all graphs. Corresponding to graph A, C and D, the final degree of saturation is about 97 %. The final point is positioned left on saturation line. In these conditions, the measured final void ratio and water content are respectively 0.76 and 28 %. This later is close the value of plastic limit (i.e., w_P=26 %).

3.2. Drying wetting path for specimens compacted at dry and wet side of SPO

Drying wetting paths of compacted specimens on dry or wet side of optimum Proctor are represented in figure 6. The drying wetting paths of SPO specimens have also been plotted in the same graphs for comparisons purposes.

By viewing the figure, it's difficult to distinguish between curves, especially in [e, log (S)] and [w, log(S)] diagrams. The main differences are observed in the others diagrams (i.e., [e, w], [Sr, log (S)], [Sr, w]. For this diagrams, the Drying wetting paths of SPO specimens, is generally positioned between the curves of specimens compacted on the dry and wet side of optimum Proctor.

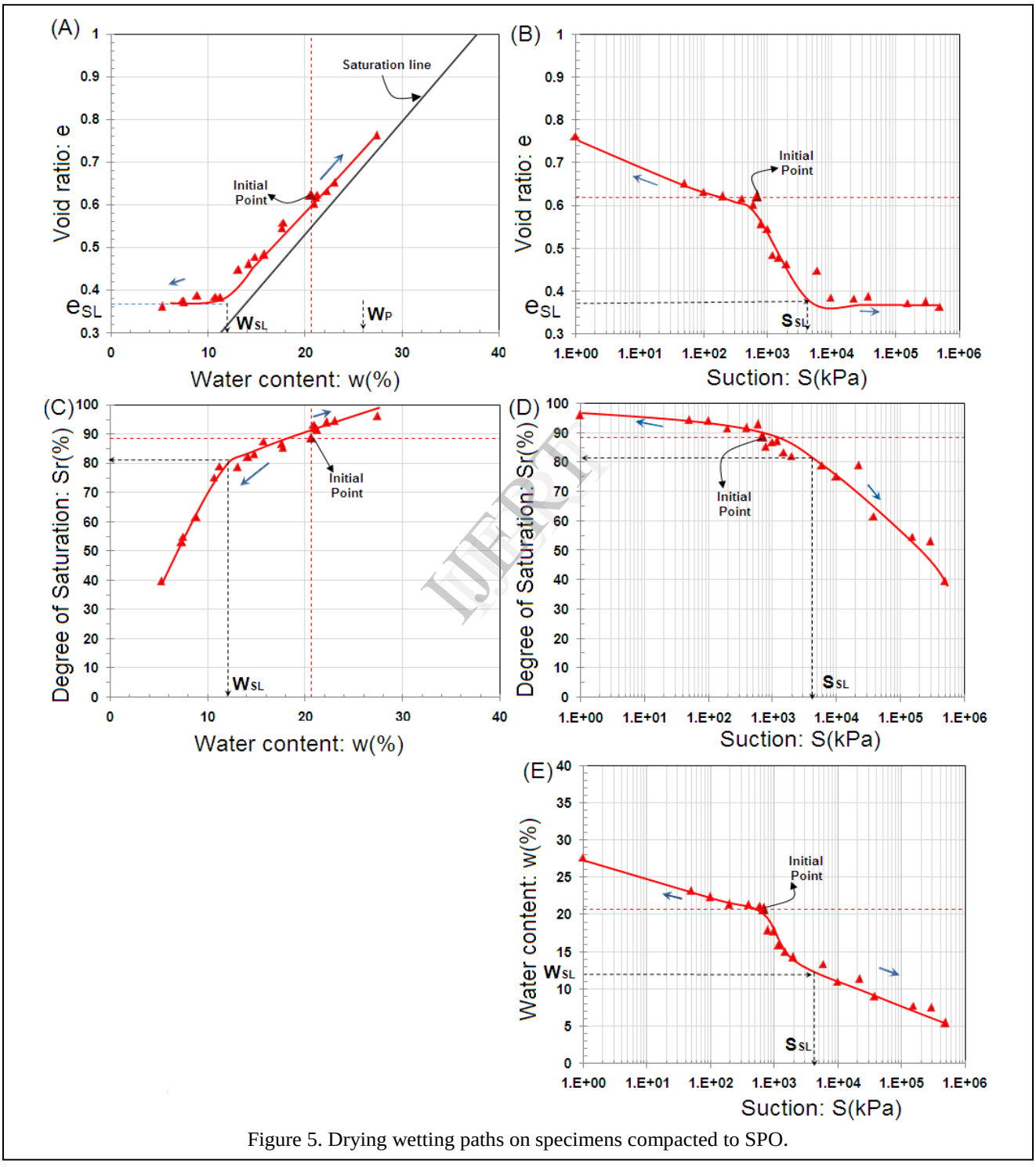

Figure 5. Drying wetting paths on specimens compacted to SPO.

Furthermore, the specimens compacted on the same side of the optimum proctor (i.e., same water content), shows that de drying wetting paths are nearly superimposed. This result confirms in part the dependence of the drying wetting paths of compacted soils to the initial water content, and indicates that for a difference of 2% in dry density, no significant different behavior is observed.

This difference can be explained by the fact that the samples compacted on the dry side have a more open

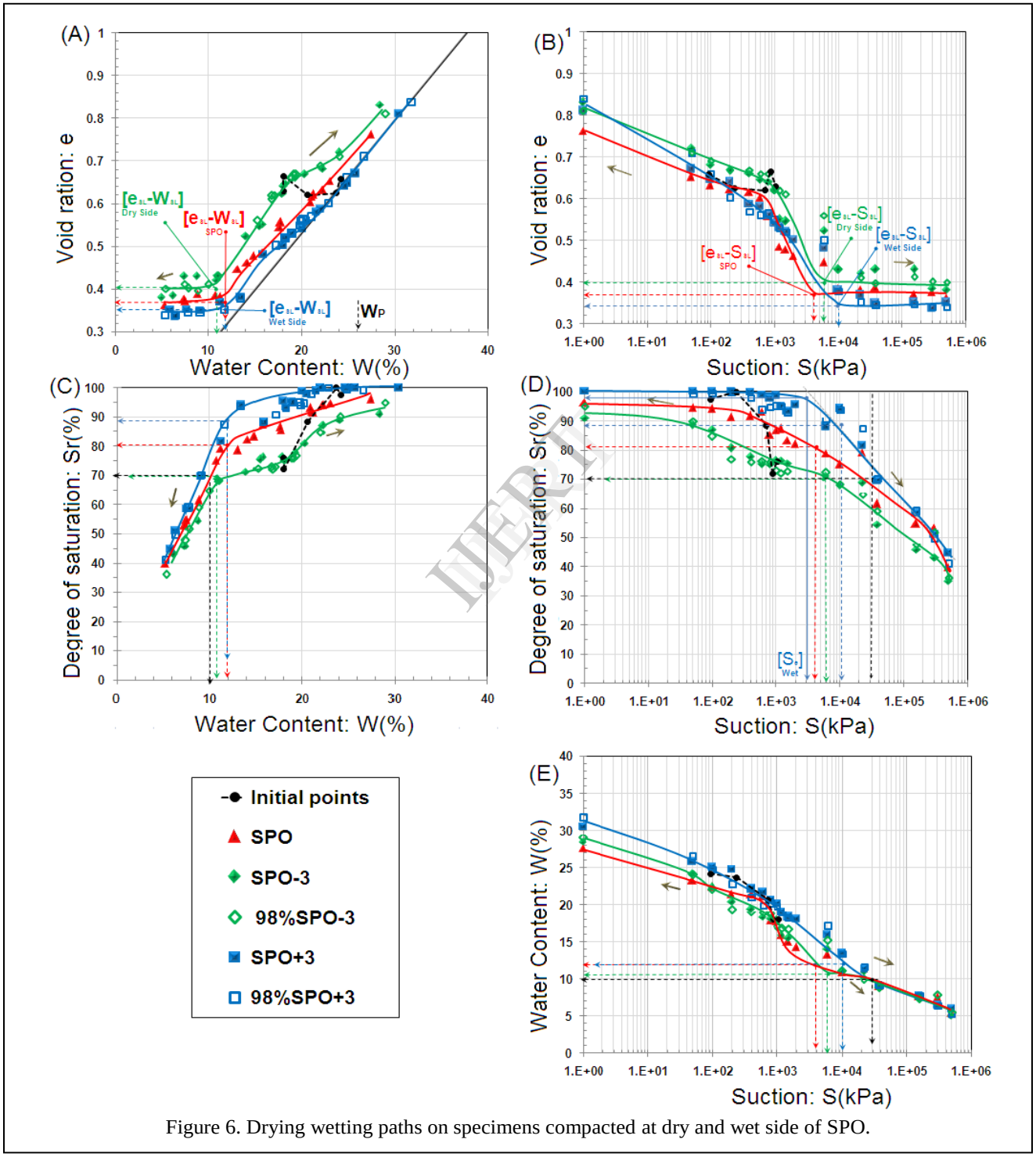

Figure 6. Drying wetting paths on specimens compacted at dry and wet side of SPO.

microstructure characterized by a bimodal porosity: inter-aggregate and intra-aggregate, contrary to the samples compacted at optimum Proctor or wet side of optimum Proctor, where their microstructure is dominated by a unimodal porosity: itra-aggregate, ([22], [24], [21]).

[8], as mentioned by [14], showed that in most clays, except smectite, the mechanism of filling or emptying of pores is obeying to a phenomenon of capillary type, governed by the law Laplace. This leads to that the samples compacted at dry side, desaturate quickly compared to the samples compacted at SPO or the wet side conditions (Diagram [Sr, log(S)], figure 6).

In the table 4, we have summarized the main characteristics on drying path, in terms of: shrinkage suction, suction of desaturation: S_e (i.e., air entry value), water content, void ratio and degree of saturation. The suction S_e is determinated in the diagram [Sr-log(S)]. It corresponds to the intersection between the line corresponding to Sr=100% and the asymptote of drying path [27]. This value was defined just for specimens compacted on the wet side of the optimum Proctor (i.e., Sr_i>97 %).

Table 4. Soil state parameters as function of suction for different initial conditions.

Initial conditions	Suction (MPa)	e	Sr (%)	w (%)
SPO	S_{SL}=4	0.37	82	12
SPO-3 98%SPO-3	S_{SL}=6	0.41	70	10.5
SPO+3	S_e=3	0.46	97	17
98%SPO+3	S_{SL}=10	0.35	89	12

The influence of the water content can be seen on the values of shrinkage suction, and the corresponding void ratio. For specimens compacted on dry side of optimum Proctor, the S_{SL} is about 6 MPa with e_{SL}=0.4, against S_{SL}=10 MPa and e_{SL}=0.35 for specimens compacted on the wet side. The optimum Proctor values range between these laters. For shrinkage limit, w_{SL}, the obtained values stay close one to the other (i.e.,10.5 % to 12 %).

We have also examined the influence of the initial dry density and water content on the drying and wetting index, (i.e., I_D and I_W), defined in the diagram [e-w], and the shrinkage and swelling potentiel, (i.e., ε_{sh} and ε_{sw}). The formula used to calculate these parameters are:

$$I_D = \frac{e_0 - e_{SL}}{w_0 - w_{SL}} \qquad (1)$$

$$I_W = \frac{e_f - e_0}{w_f + w_0} \qquad (2)$$

$$\varepsilon_{sh} = \frac{e_0 - e_{SL}}{1 + e_0} x100\% \quad (3)$$

$$\varepsilon_{sw} = \frac{e_f - e_0}{1 + e_0} x100\% \quad (4)$$

Where, w_f and e_f are respectively the final water content and void ratio obtained on wetting path.

On drying path, the drying index ranges between 0.024 to 0.033 and the shrinkage potentiel varies between 14.06 % to 22.81 % (table 5). Also, from the data given in table 5, it appears that specimens with higher initial water content expected to shrink more (low drying index and higher shrinkage potentiel). We note that in this case, the influence of initial dry density is not very clear. However, the normal and the residual shrinkage phases are identified on drying path for all compacted specimens, (figure 6, diagram [w-e)].

On wetting paths, the obtained wetting index range from 0.014 to 0.027, and the swelling potentiel from 9.37 % to 12.33 % (table 5). The highest values of wetting index are associated to specimens compacted on the wet side, and the lowest are observed on dry side. On the other hand, no tendency is observed between initial water content and swelling potentiel. However, this last, tends to increase when initial dry density increase.

Table 5. Values of drying index, wetting index, shrinkage and swelling deformation for different initial conditions.

Initial conditions	I_D	I_w	ε_{sh} (%)	ε_{sw} (%)
SPO	0.028	0.021	15.43	8.64
SPO-3	0.032	0.019	14.06	12.33
98%SPO-3	0.03	0.014	14.8	9.37
SPO+3	0.024	0.027	16.30	11.38
98%SPO+3	0.025	0.024	22.81	10.98

The comparison made in table 6 between the swelling index C_{sw}, defined as the slope of wetting path in diagram [e- log(S)], calculated for different interval of suction and the swelling index C_s, defined as the slope of unloding curve obtained from the free swell oedometer tests, indicate that for suction over than 50kPa, the values of C_{sw} are much lower than the C_s values. Approaching saturation (S≤50kPa), an increase in C_{sw} is observed, but in the most cases, they still be inferior to C_s values. This indicates that the swelling of each sample has not reached its maximum amplitude,

due to the formation of cracks during the processes of hydratation (figure 7).

Table 6. Comparison between Cws and Cs.

Initial conditions	C_{ws}		C_s
	Suction interval (kPa)		Stress interval (kPa)
	Wetting path		oedometric path
	Si-50	*50-1*	*3200-1*
SPO	0.0262	0.0647	0.075
SPO-3	0.0689	0.0647	0.07
98%SPO-3	0.0363	0.0589	0.072
SPO+3	0.0666	0.0824	0.078
98%SPO+3	0.0193	0.0765	0.078

Figure7. Example of the formation of cracks during wetting.

3.3. Drying wetting paths in the high suction range

For all the initial conditions, the drying path appears to be similar at suctions higher than 30 MPa, ($w \leq 10$ %), especially in the diagram [w- log (S)], (figure 6). The same result was obtained by other authors: [27], [9] In this range, the changes in water content as a function of the suction can be approximated by a linear equation:

$$w = -8.10^{-6} S + 9.58 \quad (5)$$

Where S is the suction given in kilopascals . The obtained regression coefficient R, is about the 0.88 (figure 9). Through this, we can say that part of the drying curve of compacted Boughrara clay can be directly deduced by simple measurement of the water content on the dry side of the optimum Proctor. The extrapolation of this conclusion to other materials requires more experimental results.

According to [27], the independence of drying path of initial conditions at low water content, means that the specimens have the same inter-aggregate structure. In other words, following to [9], at this level of suction, the drying path is mainly depends on the specific surface of the clay (mineralogical composition).

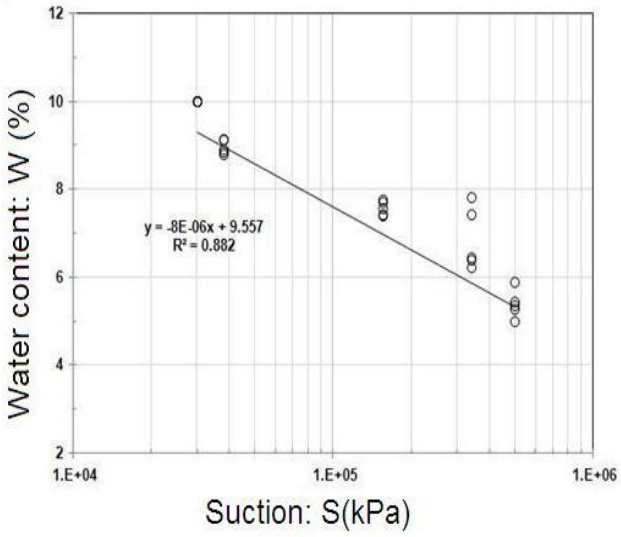

Figure 8. Adjustment of drying path of compacted specimens for suction up to 30 MPa.

4. Conclusion

The aim of this paper is to give a simplified overview of the behavior of compacted Boughrara clay on drying wetting paths, and to examine the influence of initial conditions of compaction in terms of water content and dry density in such paths. Somme interesting features have been highlighted.

- The shrinkage of compacted clay occurs in two distinct phases: normal shrinkage phase and residual shrinkage phase. The transitions between the two phases correspond to shrinkage limit: w_{SL}.
- The linearity of drying and wetting paths was observed, especially in [w-Sr] diagram.
- For the range of water content and dry density studied, the drying wetting paths was found more influenced by initial water content than the initial dry density.
- Specimens with high initial water content tend to shrink more (i.e., high shrinkage deformation, and low drying index).
- On wetting path, the influence of dry density was not clearly defined, and the swelling potentiel seems to increase with the increase of initial dry density.
- The drying path appears to be independent for initial condition of compaction for high suction range ($\geq$30MPa). At this level of suction, drying path depends mainly on adsorption property of the clay (specific surface).

References

[1] A. Hachichi, J-M. Fleureau, " Caractérisation et stabilisation de quelques sols gonflants d'Algérie", *Revue Française de Géotechnique*, N° 86, 1999, pp. 37-51.

[2] ASTM standard D 4546–03, "One-dimensional swell or settlement potential of cohesive soils", 1990, ISBN: 0-8031-2129-6. Vol 4.08, pp. 693-699.

[3] ASTM standard D 5298–94, "*Measurement of soil potential (suction) using filter paper*", 1995, ISBN: 0-80312129-6. Vol 4.09, pp. 154-159.

[4] C.W. Lauritzen, A.J. Stewart, "Soil-volunne Changes and Accompanying Moisture and Porespace Relationships", *Soil Science Society of America Journal*, 1941, pp. 113-116.

[5] D.G. Fredlund, H. Rahardjo, "*Soils mechanics for unsaturated soils*", New York: John Wiley & Sons. ISBN: 0-471-85008-X, 1993.

[6] D.G. Fredlund, A. Xing, " Equation for the soil-water characteristic curve", *Can Geotech J*, Vol 31, N°4, 1994, pp. 521-532.

[7] D.G. Fredlund, A. Xing, S.Y. Huang, "Predicting the permeability function for unsaturated soils using the soil-water characteristic curve", *Can Geotech J*, Vol 31, N°4, 1994, pp. 533-546.

[8] D. Tessier " *Étude expérimentale de l'organisation des matériaux argileux Hydratation, gonflement et structuration au cours de la dessiccation et de la réhumectation* ", Thèse de doctorat de l'université Paris 7, France.

[9] E. Romero, "*Characterization and thermo-hydro-mechanical behaviour of unsaturated boom clay : an experimental study*", PhD thesis, Universitat Politècnica de Catalunya, Barcelone, 1999.

[10] F.H. Chen, "*Foundation on expansive soils*", Elsevier, New York.

[11] F.M. Derfouf, N. Abou-Bekr, S. Taïbi, "Characterization of an Expansive Marl of the West of Algeria", In: H. Bilsel, Z. Nalbantoglu (eds) *Proceedings of International Conference on Problematic Soils GEOPROB*, Famagusta,. Eastern Mediterranean University Press, Famagusta, 25-27 May 2005, pp. 543–550.

[12] G.B. Stirk, "Some aspects of soil shrinkage and the effect cracking upon water entry into the soil", *Australian J Soil Research*, Vol 5, 1954, pp.279-290.

[13] J. Biarez, J-M. Fleureau, M.I. Zerhouni, B.S. Soepandji, "Variations de volume des sols argileux lors de cycles de drainage-humidification", *Revue Française de Géotechnique*, 1988, N° 41, pp. 63-71.

[14] J-M. Fleureau, "*Contribution à l'étude et à la modélisation du comportement des matériaux granulaires polyphasiques*", Mémoire d'habilitation à diriger des recherches, Université Pierre et Marie Curie, Paris V, 1992.

[15] J-M. Fleureau, S. Kheirbek-Saoud, R Soemitro, S. Taïbi, " Behavior of clayey soils on drying-wetting paths", *Can Geotech J*, Vol 30,1993, pp. 287-296.

[16] J-M. Fleureau, J-C. Verbrugge, R. Huergo, A.G. Correia. S. kheirbek, "Aspect of the behavior of compacted clayey soils on drying and wetting. Paths", *Can Geotech J*, Vol 39, 2002, pp. 287-296.

[17] J. Williams, C.F. Shaykewich, " An evaluation of polyethylene glycol PEG 6000 and PEG 20000 in the osmotic control of soil water matrix potential", *Can. J. Soil Science*, Vol 102, N 6, pp. 394-398.

[18] K. Lachguer, S. Taïbi., N. Abou-Bekr, " Comportement hydrique d'une argile non saturée. Application au noyau de barrage de Boughrara", *Revue Européenne de Génie civil*, Vol° 14, N 3, 2010, pp. 329-360.

[19] M. Al-Mukhtar, Y. Qi, J.F. Alcover, F. Bergaya, "Oedometric and water retention behavior of highly compacted unsaturated smectites", *Can de Geotech J*, 1999, Vol 36, pp. 675-684.

[20] M.T. Van Genuchten, "A closed form equation for predicting the hydraulic conductivity of unsaturated soils", *Soil Science Society of America Journal*, N° 44, 1980, pp. 892-898.

[21] O. Cuisinier, L. Laloui, "Fabric evolution during hydromechanical loading of a compacted silt. *International Journal for Numerical and Analytical Methods in Geomechanics*", 28, N°6, 2004, pp.483-499.

[22] P. Delage, M. Audiguier, Y-J. Cui,. D. Howat, "Microstructure of a compacted silt", *Can. Geotech. J*, Vol 33, 1996, pp.150-158.

[23] P. Delage, M.D. Howat, Y-J. Cui, "The relationship between suction and swelling properties in a heavily compacted unsaturated clay", *Engineering Geology*, Vol. 50, N°1, 1998, pp. 31-48.

[24] R. Monroy, "*The influence of load and suction changes on the volumetric behaviour of compacted London Clay*", PhD thesis, Imperial College London, 2006.

[25] R.H. Brooks, A.T. Corey, "Hydraulic properties of porous medium", *Hydrology paper*, Civil engeneering department, Colorado State University (Fort Collins), N° 03, 1964.

[26] R.W. Day. "Swell-shrink behavior of compacted clay", *Journal of Geotechnical Geoenvironmental Engineering*, 120, N° 3, 2004, pp. 618-623.

[27] S.K. Vanapalli, D.J. Fredlund, D.E, Pufahl. "The influence of soil structure and stress history on the soil-water characteristics of compacted till" *Geotechnique*,. Vol 49, N° 2, pp.143-159.

[28] S. Taïbi, J-M. Fleureau, N. Abou-Bekr, M.I. Zerhouni, A. Benchouk, K. Lachgueur, H. Souli, "Some aspects of the behaviour of compacted soils along wetting paths", *Geotechnique*, Vol 61, N 5, Thomas Telford Journals, Editions, March 2011, pp. 431 –437.

[29] W.B. Haines, " The volume changes associated with variations of water content in soil", *Journal of Agricultural Science*, N 13, 1923, pp.296-310.

[30] X. Guillot, M. Al Mukhtar, F. Bergaya, and J-M. Fleureau, "Effect of hydromechanical stresses on pore space and water retention in a clay", In *Proceedings of the 15th International Conference on Soil Mechanics and Geotechnical Engineering (ICSMGE)*, Istanbul, Turkey, Publications Committee of XV ICSMGE, A.A. Balkema, Rotterdam. Vol 1, 28-31 August 2001, pp. 101-105.

[31] Y-J. Cui, "*Étude du comportement d'un limon compacté non saturé et de sa modélisation dans un cadre élastoplastique*", Thèse de doctorat, École nationale des ponts et chaussées, France, 1993.